Implications for prediction and hazard assessment from the 2004 Parkfield earthquake

W. H. Bakun[1], B. Aagaard[1], B. Dost[2], W. L. Ellsworth[1], J. L. Hardebeck[1], R. A. Harris[1], C. Ji[3], M. J. S. Johnston[1], J. Langbein[1], J. J. Lienkaemper[1], A. J. Michael[1], J. R. Murray[1], R. M. Nadeau[4], P. A. Reasenberg[1], M. S. Reichle[5], E. A. Roeloffs[6], A. Shakal[5], R. W. Simpson[1] & F. Waldhauser[7]

Obtaining high-quality measurements close to a large earthquake is not easy: one has to be in the right place at the right time with the right instruments. Such a convergence happened, for the first time, when the 28 September 2004 Parkfield, California, earthquake occurred on the San Andreas fault in the middle of a dense network of instruments designed to record it. The resulting data reveal aspects of the earthquake process never before seen. Here we show what these data, when combined with data from earlier Parkfield earthquakes, tell us about earthquake physics and earthquake prediction. The 2004 Parkfield earthquake, with its lack of obvious precursors, demonstrates that reliable short-term earthquake prediction still is not achievable. To reduce the societal impact of earthquakes now, we should focus on developing the next generation of models that can provide better predictions of the strength and location of damaging ground shaking.

Earthquake prediction is the Holy Grail of seismology. Although the ability to predict the time and location of earthquakes remains elusive, predicting their effects, such as the strength and geographical distribution of shaking, is routine practice. The extent to which earthquake phenomena can accurately be predicted will ultimately depend on how well the underlying physical conditions and processes are understood. To understand earthquakes requires observing them up close and in detail—a difficult task because they are at present largely unpredictable, and so knowing where to put the instrumentation needed to make such observations is a challenge. The 40-km-long Parkfield section of the San Andreas fault was recognized two decades ago as a promising earthquake physics laboratory and an intensive experiment was established to record the next segment-rupturing earthquake there and provide the much-needed detailed observations. The occurrence of the anticipated moment magnitude $M_w = 6.0$ earthquake on 28 September 2004 (origin time 17:15:24 Coordinated Universal Time, UTC; epicentre location 35.815° N, 120.374° W; depth 7.9 km) fulfilled that promise.

The Parkfield section of the San Andreas fault is bounded on the northwest by a 150-km-long creeping section, where numerous small earthquakes occur, and on the southeast by hundreds of kilometres of locked fault where few earthquakes have been detected in the twentieth century (Fig. 1). The 1857 $M_w = 7.9$ Fort Tejon earthquake ruptured the locked fault southeast of Parkfield and is thought to have initiated near Parkfield[1]. On the Parkfield section, the motion of the Pacific plate relative to the North America plate is partly accommodated by repeating $M_w = 6.0$ earthquakes. The historical record of earthquakes at Parkfield includes at least six such events since 1857 (ref. 2; Supplementary Text 1, Supplementary Fig. 1 and Supplementary Table 1).

The simple setting and apparent regularity of Parkfield earthquakes[3] offered the rationale for the only scientific earthquake prediction officially recognized by the United States government[4] and an opportunity to place instruments in the region before the anticipated earthquake. The primary goal of the Parkfield Earthquake Prediction Experiment[5] was to obtain a detailed understanding of the processes leading up to the anticipated earthquake; a secondary goal was to issue a public warning shortly before the earthquake. A variety of sensors were deployed in a dense network designed specifically to record the build-up of strain in the surrounding crust, monitor earthquakes and slip on the fault, and detect any precursors that might foreshadow a large earthquake. Complementary arrays of strong-ground-motion sensors were deployed to record shaking near the earthquake rupture zone[6].

A significant development of the Parkfield experiment has been the collaboration of federal, state and local officials to develop a protocol for issuing short-term earthquake alerts[7]; the protocol provided a template for communication between scientists and emergency responders and subsequently served as a prototype for volcanic hazard warning protocols[8]. Innovations in the collection, transmission and storage of Parkfield data included a pioneering effort to provide publicly available, near-real-time earth science data streams over the internet. The systems pioneered at Parkfield have become standard elements of seismic monitoring throughout the US and have set the foundation for the installation of the USGS Advanced National Seismic System (ANSS)[9]. The Parkfield dense instrumentation network, which includes a variety of geophysical sensors, motivated the placement of a scientific borehole, Earthscope's San Andreas Fault Observatory at Depth (SAFOD), at the northwestern end of the Parkfield segment[10,11] and served as a

[1]US Geological Survey, Menlo Park, California 94025, USA. [2]Royal Netherlands Meteorological Institute (KNMI), Seismology Division, PO Box 201, 3730AE De Bilt, The Netherlands. [3]Division of Geological and Planetary Sciences, Caltech, Pasadena, California 91125, USA. [4]University of California, Berkeley Seismological Laboratory, Berkeley, California 94720, USA. [5]California Geological Survey, Sacramento, California 95814, USA. [6]US Geological Survey, Vancouver, Washington 98683, USA. [7]Lamont-Doherty Earth Observatory, Columbia University, Palisades, New York 10964, USA.

prototype for the geodetic networks that are part of Earthscope's Plate Boundary Observatory[11].

In 1985, the USGS issued a long-term prediction that an earthquake of approximately $M_w = 6$ would occur before 1993 on the San Andreas fault near Parkfield[4]. After the prediction window closed, *sans* earthquake, an independent evaluation of the Parkfield Earthquake Prediction Experiment was conducted by a Working Group of the National Earthquake Prediction Evaluation Council[12]. This working group recommended that monitoring be continued as a long-term effort to record the next earthquake at Parkfield. The failure of the long-term prediction of the time of the earthquake as well as certain aspects of the 2004 Parkfield earthquake (discussed below), have confounded nearly all simple earthquake models. However, the experiment's primary goal of observing a large earthquake near the rupture has been achieved. The instruments at Parkfield continue to operate and provide important data on postseismic deformation and other processes. Altogether, these recordings are providing a picture, at unprecedented resolution, of what occurred before, during and after the 2004 earthquake[13,14]. Although the analysis is far from complete, it is clear even now that the observations have important implications for nearly all areas of seismic hazard analysis and loss reduction.

Precursors and earthquake prediction

The idea that detectable precursory processes precede earthquakes dates back to at least the seventeenth century[15]. However, with the exception of foreshocks, unambiguous and repeatable instrumental observations of such phenomena remain elusive. As noted, identical

foreshocks preceded both the 1934 and 1966 Parkfield earthquakes by 17 min (ref. 16). However, such foreshocks did not precede the 1901 or 1922 events and so the Parkfield prediction experiment, which was designed to record potential foreshocks as well as other precursory signals, treated all precursors in a probabilistic manner[7]. At present, with the exception of an ambiguous low-level strain of $<10^{-8}$ that occurred during the 24 h before the main shock, there is no evidence of any short-term precursory signal, either seismic or aseismic[13]. Even microseismicity, detectable at the $M = 0$ threshold in the epicentral region, was absent during the six days before the main shock[13]. Notable precursory signals are not evident in the magnetic field, telluric electric field, apparent resistivity, or creep observations[13]. This lack of short-term precursors emphasizes the difficulty of reliable short-term earthquake prediction (up to a few weeks before).

Subtle strain changes of a few nanostrain were recorded on several instruments in the 24 h before the earthquake. Such changes place important constraints on earthquake nucleation physics but are too small to provide a reliable basis for issuing public warnings that a damaging earthquake is imminent. The dense instrumentation arrays continue to uncover new processes, such as deep tremor under the locked section of the fault southeast of the Parkfield segment[17]. Future hopes for prediction will rest on whether such processes are precursory or simply commonplace.

Fault structure and segment boundaries

The similar magnitude and rupture extent of the last six Parkfield earthquakes supports the concept of fault segmentation and the role of segment boundaries in influencing the rupture extent and magnitude of earthquakes. The nature of segment boundaries, however, is controversial. Fault geometry, rheological and frictional properties of materials, pore fluids and stress conditions have all been proposed to explain segment boundaries[18].

Lindh and Boore[19] suggested a fault-geometry-based explanation for the location of the boundaries of the Parkfield segment: a 5° bend in the fault trace to the northwest and a right-stepover to the southeast appeared to offer geometric obstacles that could limit earthquake rupture. The 2004 aftershocks relocated with a three-dimensional velocity model do not appear to show these features extending to depth (Fig. 2). Aftershocks and earlier seismicity[20] at depths below 6–7 km seem to be confined to a narrow band (see Supplementary Fig. 4). Because the fault seems straighter at depth, where large Parkfield earthquakes nucleate, than it does at the surface, it is possible that fault geometry is not the controlling factor in the location of the Parkfield segment boundaries[20]. However, the complex surface trace geometry may result from deformation associated with the segment boundaries at seismogenic depth. That is, irregularities in the surface trace may reflect the presence of the boundaries at depth rather than being the primary cause of these boundaries.

An alternative explanation for the boundaries of the Parkfield segment is based on fault zone rheology. This segment is adjoined on the northwest by a creeping section where, perhaps, stable sliding precludes large earthquakes and on the southeast by a locked section, which may fail only in infrequent great earthquakes[19,21]. The reasons for creep to the northwest and locking to the southeast are not clear. Properties of materials and fluid overpressure adjacent to the fault have been proposed to explain creeping and locked fault segments[20,22]. A better knowledge of the materials and conditions within the fault zone obtained from SAFOD[10] should help to discriminate between these possibilities. Ultimately, a combination of factors, including deep fault geometry, fault rheology, and stress level, may be necessary to explain why a fault creeps or is locked and what constitutes a segment boundary.

Seismic and aseismic slip

Over the long term, both seismic and aseismic slip along plate
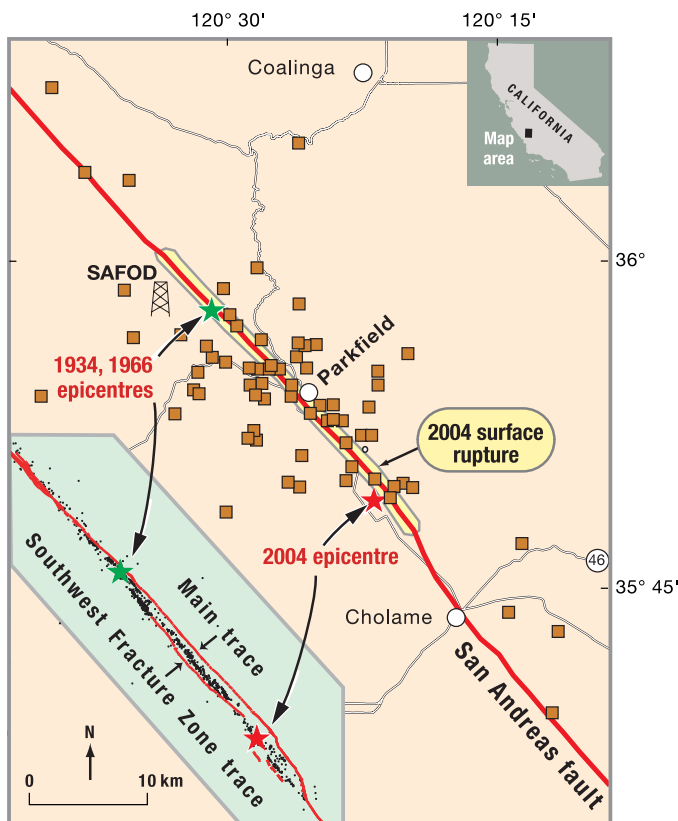

Figure 1 | Location of the 2004 Parkfield earthquake. The zone of surface rupture (yellow) is shown along the San Andreas fault (red lines). Locations of seismographs, strainmeters, creepmeters, magnetometers, and continuous GPS stations shown as squares. The strong-motion sensors (not shown here) are located on Fig. 4. Lower inset (same scale, in pale green) shows epicentres of 2004 aftershocks (black dots) plotted relative to fault traces[30]. Upper inset, map location.

boundaries like the San Andreas fault accommodate the relative motion between the plates. To apply even the simplest mechanical model for the build-up of strain and its sudden release in earthquakes, one must account for slip on the fault that occurs aseismically. Aseismic slip has been recognized as a potentially important component of the slip budget on strike-slip faults in the San Francisco Bay area[23] and on megathrust faults along subduction plate boundaries in the Pacific Northwest region of the United States[24] and in Japan[25]. How seismic and aseismic slip are distributed over a fault and how much and where aseismic slip occurs during the times between large earthquakes are, however, not well resolved. Measurements of slip beginning shortly after the 1966 Parkfield earthquake[13,26] appear to provide some insight into these questions. The region of maximum slip in the 2004 event appears to partially fill a deficit in the distribution of slip that had accumulated beginning with the 1966 earthquake[13], but some slip-deficient regions apparently remain (Fig. 3).

Postseismic surface slip of 35–45 cm was observed using alinement arrays following the 1966 Parkfield earthquake[27]. The 2004 Parkfield event, however, is the first at this location for which the geodetic data were recorded during and after the earthquake with sufficient temporal and spatial resolution to enable separation of the coseismic and postseismic signals. Postseismic slip equal to about 60% of the coseismic slip occurred in the first month after the 2004 event (Fig. 3f). Alinement array data from the 2004 earthquake suggest that near-surface slip will reach 20–50 cm over the next 2–5 yr (ref. 28), comparable to what was seen after the 1966 event[27]. Additionally, the Global Positioning System (GPS) data suggest that postseismic effects may persist for a decade, and that ultimately, the slip associated with this earthquake (coseismic plus postseismic) will balance the estimated slip deficit that existed on the fault at the time of the earthquake.
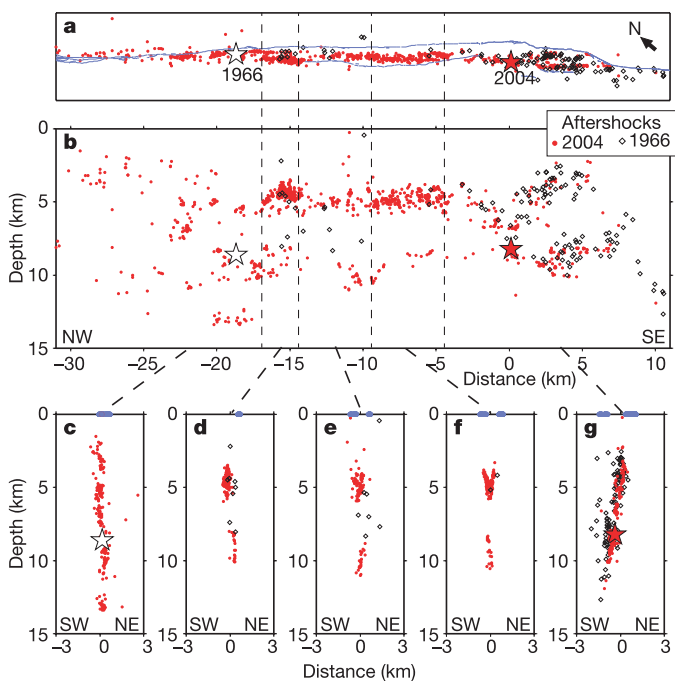
Prediction of damaging ground motion

Most of the catastrophic damage in earthquakes occurs close to the earthquake source, but relatively few recordings of strong shaking close to an earthquake have been made. The ground motion near the 2004 earthquake[29] was recorded at eight sites within 1 km of the rupture and at 40 sites between 1 and 10 km from the rupture (Fig. 4), nearly doubling the global data set of strong-motion records within those distances. These records show the wavefield in unprecedented detail[14] and reveal large spatial variations in shaking amplitude.

The peak horizontal acceleration (PGA) for two of the records are greater than 1.0g (where g is the acceleration due to gravity) with one of these exceeding the instrument's recording capacity of 2.5g. Recordings of accelerations greater than 1g are rare, but they may not be anomalous at locations within a few kilometres of fault ruptures. Preliminary seismic slip models (see Fig. 3d for example) indicate slip was concentrated in two small regions, near the stations recording the strongest PGA. The local stress drop in these regions of concentrated slip appears to be more than an order of magnitude larger than the average stress drop of 0.2 MPa associated with the very smooth geodetic slip model (Fig. 3d). Temporal variations in rupture propagation, however, probably also influenced the radiation of the strongest shaking, as illustrated by the spatial variability in PGA (Fig. 4) and peak ground velocity close to the fault. Explaining the large variations in amplitude over distances of just a few kilometres continues to challenge our understanding of earthquake rupture dynamics and our ability to predict ground motions near the rupture (Fig. 4b and Supplementary Fig. S3).

Spatial variations in the intensity of shaking, such as peak ground acceleration and peak ground velocity, are often attributed to four factors: differences in soil conditions among sites, differences in the
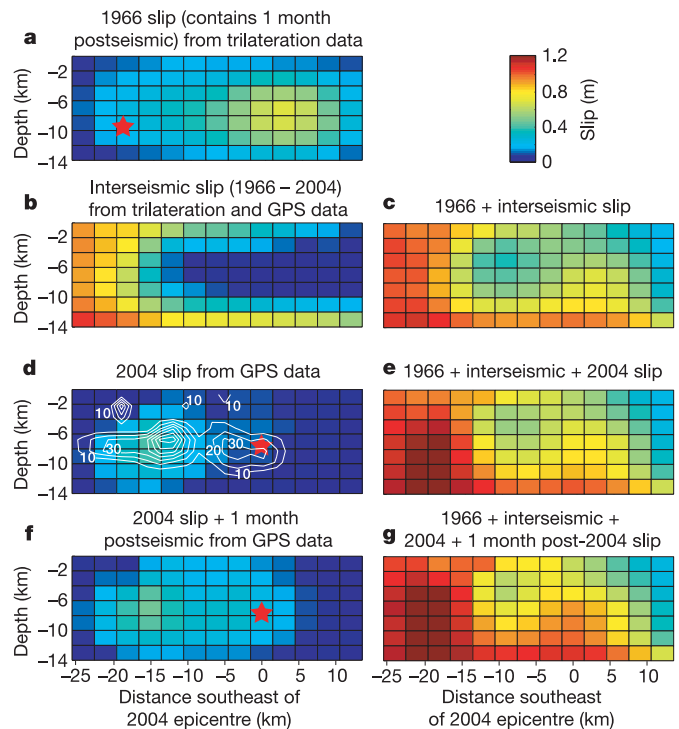

Figure 2 | Spatial distribution of Parkfield aftershocks. Locations are listed in Supplementary Table S2. Aftershocks in 2004 are shown as red dots, those in 1966 as black diamonds. Aftershocks were relocated (Supplementary Text 3) using a three-dimensional velocity model[48] and the double difference relocation technique[44]. San Andreas fault traces (purple lines) and the 1966 (open star) and the 2004 (red star) main shock hypocentres are also shown. **a**, Map view. **b**, Along-fault section. **c–g**, Cross sections for the fault sections shown in **a** and **b**. The purple dots at zero depth indicate the traces shown in **a**. The aftershocks in **f** reveal multiple strands[49] activated by the main shock.

Figure 3 | Distribution of slip on the San Andreas fault since 1966 estimated from geodetic data. a, **b**, **d**, **f**, Slip; **c**, **e**, **g**, accumulated slip. Slip in the 2004 earthquake (**d**) concentrated near an area with an apparent slip deficit (compare **c** and **d**). In **d** we overlay contours of slip, estimated using both geodetic and seismologic data, giving a higher-resolution image of the slip distribution with a peak slip of 77 cm (ref. 50). These slip models illustrate how slip in earthquakes (coseismic and postseismic) combines with aseismic slip between earthquakes to generate the cumulative offset across the fault. Slip values are listed in Supplementary Table S3.

wave propagation to the sites, complexities of the rupture geometry, and heterogeneity of slip on the fault. Analysis of the strong-motion records from the 2004 earthquake should lead to a fuller understanding of how each of these factors contributes to the spatial variability in strong shaking, especially at locations close to the fault rupture. This has significant ramifications for earthquake hazard research. For example, the variability in PGA was greatest close to the rupture (Fig. 4). This suggests that complexities in the seismic source may have been the primary cause of the variations, in which case research with a greater emphasis on understanding the physical processes controlling complexity of the source would be most effective. On the other hand, near-surface soil conditions at the site

and heterogeneity in the properties of the Earth's crust that influence seismic-wave propagation are known to be important for determining the shaking at locations farther from the rupture. If these factors are found to be important for predicting the distribution of shaking within a few kilometres of the rupture as well, then directing additional resources towards developing detailed maps of these properties would also be effective. The large uncertainties in current estimates of strong ground shaking require that societal guidelines, including the Uniform Building Code and California's Alquist-Priolo Fault Zoning Act[30], be conservative, thereby driving up the cost of construction and hazard mitigation. To the extent that such variations in shaking are predictable, the precision of seismic hazard maps and building codes could be improved, allowing necessarily limited hazard mitigation funds to be used more effectively.
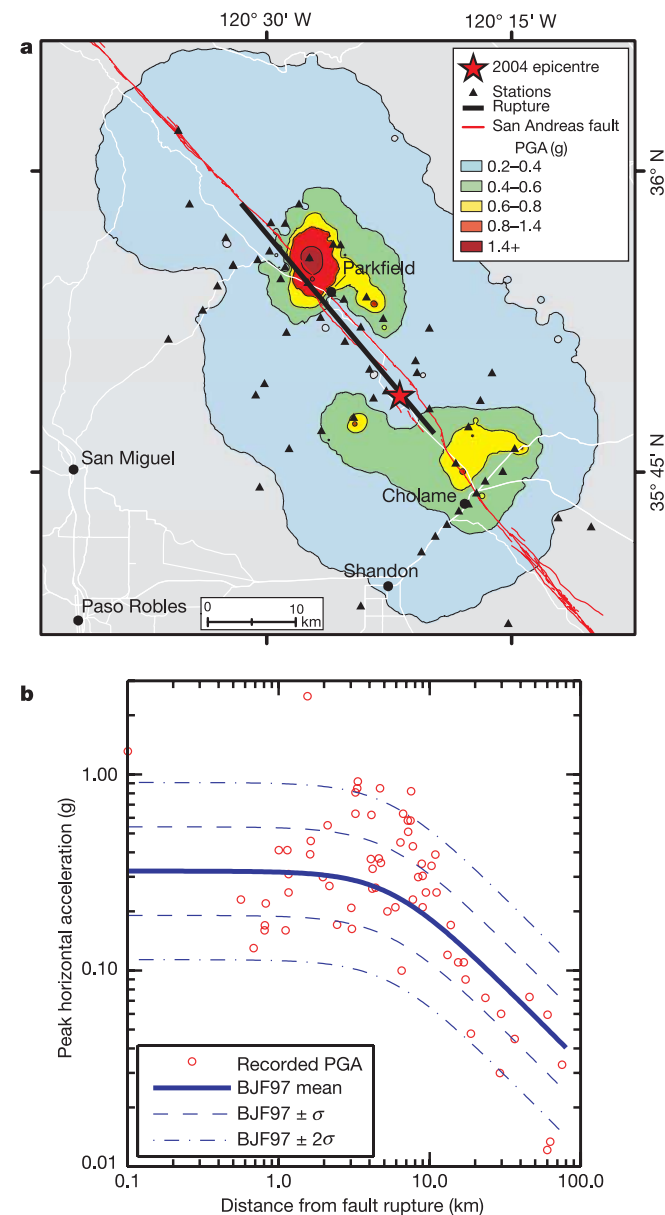
Long-term non-randomness of earthquakes

The notion that large earthquakes tend to occur as similar-size 'characteristic' events on fixed segments of a fault and that these segments are identifiable from geologic and geophysical data arose in the 1980s (refs 3, 19 and 31) and remains central to fault-based Probabilistic Seismic Hazard Analysis (PSHA). PSHA also includes other approaches such as smoothed seismicity models (see ref. 32), random events and multiple segment ruptures (see ref. 23). The sequence of earthquakes at Parkfield since 1857 has long been considered a prime example of the recurrence of a characteristic earthquake[3,5,23]. Two classes of characteristic earthquakes have been considered for these events. In the first, events have the same faulting mechanism and magnitude, and occur on the same fault segment[31]; this class of characteristic behaviour is most appropriate for long-term forecasting of earthquakes and is often inferred from paleoseismic investigations. In the second class, the events also have the same epicentre and rupture direction[3]. If events in the second class were further constrained to have the same rupture time history and distribution of slip, then this class of recurrent behaviour would imply low variability in the distribution of recurrent strong ground shaking among the recurrences of characteristic events.

The 1934, 1966 and 2004 Parkfield earthquakes are remarkably similar in size (see Fig. 5 for example) and location of rupture, albeit not in epicentre or rupture propagation direction. The aftershocks of the 1966 and 2004 earthquakes delineate many of the same fault structures (Fig. 2). Furthermore, most of the observations available for the Parkfield earthquakes in 1881, 1901 and 1922 are consistent with the hypothesis that these earlier earthquakes were similar in size and general location to the later events[3,5]. Owing to limited observations of these earlier events, a rigorous definition of the Parkfield main shocks must be limited to their overall size and their location based on rupture along the Parkfield segment[33]. Michael and Jones' definition[33] was designed to encompass the Parkfield main shocks through 1966; the 2004 main shock also satisfies their definition. Thus, the Parkfield earthquakes are consistent with the first class of characteristic earthquake behaviour. However, the variability in the spatial distribution of slip for the last three events[34,35] and the different direction of rupture propagation in the 2004 event invalidates the application of the second class of characteristic behaviour to the Parkfield earthquakes.

We note that the six Parkfield earthquakes since 1857 have occurred with statistically significant (albeit imperfect) regularity in time—more regular than random but not sufficiently periodic to be predictable in any useful way beyond long-term statistical forecasts (Supplementary Text 2). This limited regularity underlies most of the long-term prediction models proposed for the earthquakes[3,5]. The departures from perfectly regular occurrence of these earthquakes have been interpreted using physics-based variations upon the characteristic earthquake model. For example, the Parkfield Recurrence Model, used at the outset of the experiment in 1985, assumed a constant fault loading rate and failure threshold and allowed that main shocks could be triggered early by foreshocks, but

Figure 4 | Horizontal PGA from ShakeMap[51]. a, Map view. Station locations shown by triangles. The thin red line delineates the Alquist-Priolo fault traces[30] and the thick black line is the fault trace based on aftershock locations. **b**, Horizontal PGA as a function of distance from the fault rupture. The distances are based on the approximate projection of the fault to the ground surface. The mean (solid line) and $\pm 1\sigma$ (dashed lines) and $\pm 2\sigma$ (dash-dotted lines) for the Boore–Joyner–Fumal 1997 attenuation relation[52] are shown. The PGA which exceeded the 2.5*g* limit of the instrument is plotted at 2.5*g*.

did not allow for late events[5]. Consequently, it has been invalidated by the long time interval between the 1966 and 2004 main shocks. In a time-predictable model, the time between successive events is proportional to the slip of the prior event; in a slip-predictable model, the size of an earthquake is proportional to the time since the prior event[36]. Neither of these models is compatible with the sequence of Parkfield earthquake ruptures[34]. Various forms of fault interaction have been proposed to explain the variation in recurrence intervals of the earthquakes[37].

Statistical models of earthquake recurrence have also been applied to these events. The variability in the time between earthquakes implies a coefficient of variability (COV) of about 0.45 which is similar to the COV used in recent forecasts for the San Francisco Bay Area[23] but greater than that proposed in earlier models for the Parkfield sequence[38]. Earthquake activity over a wide range of smaller magnitudes ($M_w = 0$ to 5) also occurs at Parkfield. Clusters of microearthquakes that produce nearly identical waveforms repeatedly rupture small, fixed patches of the fault—some with remarkable regularity. Many of these clusters have characteristic recurrence times of months to years that scale with the magnitude of the repeating events. Changes in this recurrence time have been used to infer that slip rates over portions of the fault vary with time[39]. Similar to the Parkfield main shocks, models of these events suggest that they may balance their local slip budget with a mix of seismic and aseismic slip[40].

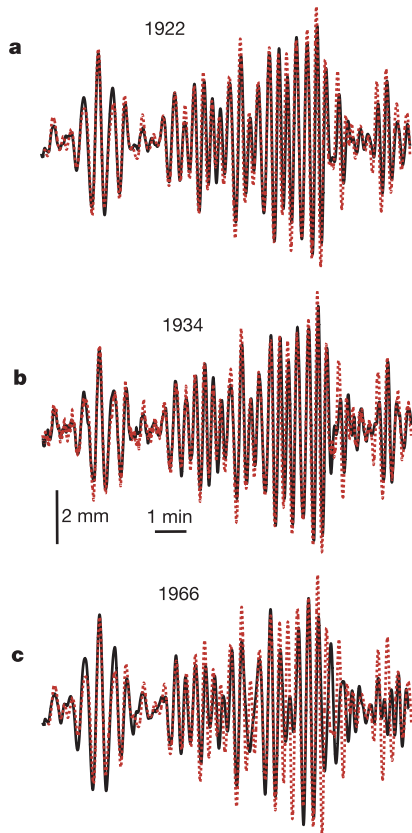The earthquakes at Parkfield, both large and small, provide a fertile

Figure 5 | Seismograms for Parkfield earthquakes at De Bilt, the Netherlands. North–south seismogram for the 2004 Parkfield earthquake (red dashed line) is plotted relative to the 1922, 1934, and 1966 Parkfield earthquakes in **a**, **b**, and **c** respectively. The 1922, 1934, and 1966 events were recorded by horizontal Galitzin seismographs. The 2004 signal, recorded by a three-component, broadband digital station located at the same site as the Galitzin seismograph, was digitally filtered to simulate a Galitzin seismograph. The similar amplitudes and waveforms imply the same seismic moment, focal mechanism, and teleseismic wave path.

laboratory for testing and refining the characteristic earthquake concept by offering information on slip distribution, rupture dynamics and afterslip, and for testing models of earthquake recurrence and interaction, which are central to contemporary earthquake hazard assessment[23]. (The characteristic earthquake model can also be tested using global data sets. Kagan and Jackson[41] concluded that too few of Nishenko's[42] predicted gap-filling circum-Pacific earthquakes occurred in the first 5 yr.) Although the Parkfield earthquake history supports the use of characteristic events for earthquake forecasting, this topic remains controversial[42,43] and we must consider whether conclusions drawn from observations at Parkfield will transfer to other seismogenic regions. For instance, does the presence of aseismic slip to the north of and within the Parkfield segment yield unusual earthquake behaviour? Observations of the large amount of postseismic slip following the 2004 earthquake suggest that it may help to balance the slip budget. Faults that do not slip aseismically may exhibit more irregular behaviour because other large events are needed to balance the slip budget. There are other faults, however, with aseismic slip that produce small repeating events and may thus produce characteristic events similar to those observed at Parkfield. These include the Hayward and Calaveras faults in California and partially coupled subduction zones[44–46].

Implications for future research

The magnitude and rupture extent of the 2004 Parkfield earthquake were correctly anticipated, but its time of occurrence clearly was not. This suggests that long-term earthquake forecasts require models that include higher degrees of variability (for example, see ref. 23). Although the 2004 Parkfield earthquake was ideally located within a dense monitoring network specifically designed to detect foreshocks and other possible short-term precursors, no significant signals were detected. This documented absence of clear precursory activity sets stringent bounds on the processes that preceded this earthquake. Attempts to detect short-term precursory strain changes near several other recent $M_w = 5.3–7.3$ earthquakes in California and Japan have also failed[47]. These experiences demonstrate that reliable short-term earthquake prediction (up to a few weeks in advance) will be very difficult at best. Although the search for precursors should not be abandoned, we should thoroughly explore other ways to mitigate losses in earthquakes.

Earthquake loss mitigation begins with hazard assessment. Improved hazard assessment will require incorporating the observed variability in both earthquake sources and the resulting ground motions into probabilistic seismic hazard analysis. The history of events at Parkfield and the detailed observations of the 2004 event have revealed variability in intervals between earthquakes, variations in slip distributions of large events, and spatial variations in strong ground motion. Incorporating realistic variability into hazard assessments will entail sophisticated three-dimensional numerical models that can accurately explore many seismic cycles and include the build-up of strain via plate motions, dynamic stress changes during rupture, and postseismic deformation. Such models must be able to explain the interaction of aseismic and seismic slip, the segmentation of faults, and the strong spatial variations in the intensity of strong shaking. Complementary data from *in situ* studies of the Earth's crust, such as SAFOD[10], laboratory experiments that recreate the conditions of faults in the Earth, and continued seismic monitoring will be needed to constrain the numerical models.

The value of the unique long-term record of crustal deformation being collected at Parkfield suggests that the monitoring there should continue. Parkfield-like experiments embedded within broader monitoring networks in other locations can provide similarly valuable data for faults in other tectonic contexts. Additional selected faults in California, which are already contained within sparse monitoring networks, should be densely instrumented. Large earthquakes are also anticipated on known fault segments in China, Japan, Turkey and elsewhere, and international cooperation should be

sought to develop comprehensive monitoring in these regions. The Parkfield experiment showed that diligence is required to maintain these specialized networks until a large earthquake occurs, and the detailed observations made at Parkfield demonstrate how valuable such perseverance can be for advancing our understanding of earthquakes.

1. Sieh, K. E. Slip along the San Andreas Fault associated with the great 1857 earthquake. *Bull. Seismol. Soc. Am.* **68**, 1421–1447 (1978).
2. Toppozada, T. R., Branum, D. M., Reichle, M. S. & Hallstrom, C. L. San Andreas fault zone, California; M ≥ 5.5 earthquake history. *Bull. Seismol. Soc. Am.* **92**, 2555–2601 (2002).
3. Bakun, W. H. & McEvilly, T. V. Recurrence models and Parkfield, California, earthquakes. *J. Geophys. Res.* **89**, 3051–3058 (1984).
4. Shearer, C. F. Southern San Andreas fault geometry and fault zone deformation: implications for earthquake prediction (National Earthquake Prediction Council Meeting, March, 1985). *US Geol. Surv. Open-file Rep.* **85–507**, 173–174 (USGS, Reston, Virginia, 1985).
5. Bakun, W. H. & Lindh, A. G. The Parkfield, California, earthquake prediction experiment. *Science* **229**, 619–624 (1985).
6. Sherburne, R. W. Ground shaking and engineering studies near the San Andreas fault zone. *Calif. Geol.* **41**, 27–32 (1988).
7. Bakun, W. H. *et al.* Parkfield, California, earthquake prediction scenarios and response plans. *US Geol. Surv. Open-file Rep.* **87–192**, 1–45 (USGS, Reston, Virginia, 1987).
8. Hill, D. P. *et al.* Response plans for volcanic hazards in the Long Valley caldera and Mono Craters area, California. *US Geol. Surv. Open-file Rep.* **91–270**, 1–64 (USGS, Reston, Virginia, 1991).
9. USGS *Advanced National Seismic System* ⟨http://earthquake.usgs.gov/anss/⟩ (USGS Earthquake Hazards Program, 2000).
10. Hickman, S., Zoback, M. & Ellsworth, W. Introduction to the special section: preparing the San Andreas Fault Observatory at depth. *Geophys. Res. Lett.* **31**, L12S01, doi:10.1029/2004GL020688 (2004).
11. Earthscope Project *Exploring the Structure and Evolution of the North American Continent* ⟨http://www.earthscope.org/⟩ (2003).
12. National Earthquake Prediction Evaluation Council Working Group. Earthquake research at Parkfield, California, 1993 and beyond—report of the NEPEC working group to evaluate the Parkfield earthquake prediction experiment. *US Geol. Surv. Circ.* **1116**, 1–14 (USGS, Reston, Virginia, 1994).
13. Langbein, J. *et al.* Preliminary report on the 28 September 2004, M6.0 Parkfield, California, earthquake. *Seismol. Res. Lett.* **76**, 10–26 (2005).
14. Shakal, A. *et al.* Preliminary analysis of strong-motion recordings from the 28 September 2004 Parkfield, California earthquake. *Seismol. Res. Lett.* **76**, 27–39 (2005).
15. Rikitake, T. *Earthquake Prediction* 7–26 (Elsevier, Amsterdam, Netherlands, 1976).
16. Bakun, W. H. & McEvilly, T. V. Earthquakes near Parkfield, California; comparing the 1934 and 1966 sequences. *Science* **205**, 1375–1377 (1979).
17. Nadeau, R. M. & Dolenc, D. Nonvolvanic tremors deep beneath the San Andreas fault. *Science* **307**, 389, doi:10.1126/science.1107142 (2004).
18. Harris, R. A. Numerical simulations of large earthquakes: Dynamic rupture propagation on heterogeneous faults. *Pure Appl. Geophys.* **161**, 2171–2181, doi:10.1007/s00024–004–2556–8 (2004).
19. Lindh, A. G. & Boore, D. M. Control of rupture by fault geometry during the 1966 Parkfield earthquake. *Bull. Seismol. Soc. Am.* **71**, 95–116 (1981).
20. Eberhart-Phillips, D. & Michael, A. J. Three-dimensional velocity structure, seismicity, and fault structure in the Parkfield region, Central California. *J. Geophys. Res.* **98**, 15737–15758 (1993).
21. Liu, J., Klinger, Y., Sieh, K. & Rubin, C. Six similar sequential ruptures of the San Andreas Fault, Carrizo Plain, California. *Geology* **32**, 649–652 (2004).
22. Irwin, W. P. & Barnes, I. Effect of geologic structure and metamorphic fluids on seismic behaviour of the San Andreas fault system in central and northern California. *Geology* **3**, 713–716 (1975).
23. Working Group on California Earthquake Probabilities. Earthquake probabilities in the San Francisco Bay region: 2002–2031. *US Geol. Surv. Open-file Rep.* **03–214**, 1–340 (USGS, Reston, Virginia, 2003).
24. Dragert, H., Wang, K. L. & James, T. S. A silent slip event on the deeper Cascadia subduction interface. *Science* **292**, 1525–1528 (2001).
25. Kawasaki, I. *et al.* The 1992 Sanriku-Oki, Japan, ultra-slow earthquakes. *J. Phys. Earth* **43**, 105–116 (1995).
26. Harris, R. A. & Segall, P. Detection of a locked zone at depth on the Parkfield, California segment of the San Andreas fault. *J. Geophys. Res.* **92**, 7945–7962 (1987).
27. Lienkaemper, J. J. & Prescott, W. H. Historic surface slip along the San Andreas fault near Parkfield, California. *J. Geophys. Res.* **94**, 17647–17670 (1989).
28. Lienkaemper, J. J., Baker, B. & McFarland, F. S. Slip in the 2004 Parkfield, California earthquake measured on alinement arrays. *Eos* **85**(47), Abstr. S54B–01 (2004).
29. CISN *Strong Motion Engineering Data Center* ⟨http://www.quake.ca.gov/cisn-edc/⟩ (2000).
30. California Geological Survey *Alquist-Priolo Earthquake Fault Zones* ⟨http://www.consrv.ca.gov/CGS/rghm/ap/⟩ (1998).
31. Schwartz, D. P. & Coppersmith, K. J. Fault behaviour and characteristic earthquakes; examples from the Wasatch and San Andreas fault zones. *J. Geophys. Res.* **89**, 5681–5698 (1984).
32. Frankel, A. D. *et al.* USGS national seismic hazard maps. *Earthq. Spect.* **16**, 1–19 (2000).
33. Michael, A. J. & Jones, L. M. Seismicity alert probabilities at Parkfield, California, revisited. *Bull. Seismol. Soc. Am.* **88**, 117–130 (1998).
34. Murray, J. R. & Segall, P. Testing time-predictable earthquake recurrence by direct measure of strain accumulation and release. *Nature* **419**, 287–291 (2002).
35. Segall, P. & Du, Y. How similar were the 1934 and 1966 Parkfield earthquakes? *J. Geophys. Res.* **98**, 4527–4538 (1993).
36. Shimazaki, K. & Nakata, T. Time-predictable recurrence model for large earthquakes. *Geophys. Res. Lett.* **7**, 279–282 (1980).
37. Ben-Zion, Y., Rice, J. R. & Dmowska, R. Interaction of the San Andreas fault creeping segment with adjacent great rupture zones, and earthquake recurrence at Parkfield. *J. Geophys. Res.* **98**, 2135–2144 (1993).
38. Savage, J. C. The Parkfield Prediction Fallacy. *Bull. Seismol. Soc. Am.* **83**, 1–6 (1993).
39. Nadeau, R. M. & McEvilly, T. V. Fault slip rates at depth from recurrence intervals of repeating earthquakes. *Science* **285**, 718–721 (1999).
40. Beeler, N. M., Lockner, D. A. & Hickman, S. H. A simple creep-slip and stick-slip model for repeating earthquakes and its application to micro-earthquakes at Parkfield. *Bull. Seismol. Soc. Am.* **91**, 1797–1804 (2001).
41. Kagan, Y. Y. & Jackson, D. D. New seismic gap hypothesis: Five years after. *J. Geophys. Res.* **100**, 3943–3959 (1995).
42. Nishenko, S. P. Circum-Pacific seismic potential—1989–1999. *Pure Appl. Geophys.* **135**, 169–259 (1991).
43. Main, I. *Is reliable earthquake prediction of individual earthquakes a realistic scientific goal?* ⟨http://www.nature.com/nature/debates/earthquake/equake_contents.html⟩ (Nature Debate 25 February to 8 April 1999).
44. Waldhauser, F. & Ellsworth, W. L. A double-difference earthquake location algorithm; method and application to the northern Hayward Fault, California. *Bull. Seismol. Soc. Am.* **90**, 1353–1368 (2000).
45. Schaff, D. P., Beroza, G. C. & Shaw, B. E. Post-seismic response of repeating earthquakes. *Geophys. Res. Lett.* **107**, B9, doi:10.1029/2001JB000633 (1998).
46. Uchida, N., Matsuzawa, T., Igarashi, T. & Hasegawa, A. Interplate quasi-static slip off Sanriku, NE Japan, estimated from repeating earthquakes. *Geophys. Res. Lett.* **30**, doi:10.1029/2003GL017452 (2003).
47. Johnston, M. J. S. & Linde, A. T. Implications of crustal strain during conventional, slow, and silent earthquakes. *Int. Handbk Earthq. Eng. Seismol.* **81A**, 589–605 (2002).
48. Michael, A. J. & Eberhart-Phillips, D. M. Relations among fault behaviour, subsurface geology, and three-dimensional velocity models. *Science* **253**, 651–654 (1991).
49. Waldhauser, F., Ellsworth, W. L., Schaff, D. P. & Cole, A. Streaks, multiplets, and holes: high-resolution spatio-temporal behaviour of Parkfield seismicity. *Geophys. Res. Lett.* **31**, L18608, doi:10.1029/2004GL020649 (2004).
50. Ji, C., Choi, K. K., King, N., Larson, K. M. & Hudnut, K. W. Co-seismic slip history and early afterslip of the Parkfield earthquake. *Eos* **85**(47), Abstr. S53D–04 (2004).
51. CISN ShakeMap. *Estimated Instrumental Intensity* ⟨http://www.quake.ca.gov/shake/index.html⟩ (1997).
52. Boore, D. M., Joyner, W. B. & Fumal, T. E. Equations for estimating horizontal response spectra and peak acceleration from Western North American earthquakes: A summary of recent work. *Seismol. Res Lett.* **68**, 128–153 (1997).